Environmental Science & Technology

ARTICLE

pubs.acs.org/est

Adsorption and Surface Complexation Study of L-DOPA on Rutile (α-TiO_2) in NaCl Solutions

Salima Bahri,[†] Caroline M. Jonsson,[‡,§] Christopher L. Jonsson,[‡,§] David Azzolini,[‡] Dimitri A. Sverjensky,[*,‡,§] and Robert M. Hazen[§]

[†]Department of Chemistry, Barnard College, New York, New York 10027, United States

[‡]Department of Earth & Planetary Sciences, Johns Hopkins University, Baltimore, Maryland 21218, United States

[§]Geophysical Laboratory, Carnegie Institution of Washington, 5251 Broad Branch Road NW, Washington, D.C. 20015, United States

Supporting Information

ABSTRACT: Dihydroxyphenylalanine (DOPA) and similar molecules are of considerable interest in studies of bioadhesion to minerals, solar cells involving titanium dioxide, and biomedical imaging. However, the extent and mechanisms of DOPA adsorption on oxides in salt solutions are unknown. We report measurements of DOPA adsorption on well-characterized rutile (α-TiO_2) particles over a range of pH, ionic strength, and surface coverage as well as a surface complexation model analysis establishing the stoichiometry, model surface speciation, and thermodynamic equilibrium constants, which permits predictions in more complex systems. DOPA forms two surface species on rutile, the proportions of which vary strongly with pH but weakly with ionic strength and surface loading. At pH < 4.5 a species involving four attachment points ("lying down") is important, whereas at pH > 4.5 a species involving only two attachment points via the phenolic oxygens ("standing up") predominates. Based on evidence of strong attachment of DOPA to titanium dioxide from single molecule AFM (Lee, H. et al., *Proc. Natl. Acad. Sci.* **2006**, *103*, 12999−12003) and studies of catechol adsorption, one or more of the DOPA attachments for each species is inner-sphere, the others are likely to be H-bonds.

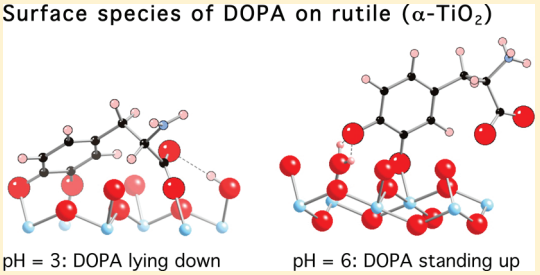

INTRODUCTION

The interactions between aqueous amino acids and mineral surfaces are of interest in a great variety of fields from biomineralization to theories of the origin of life. In bioadhesion studies, the catecholic amino acid 3,4-dihydroxyphenylalanine (DOPA) has been indentified as an important molecule in bioadhesive proteins such as those used by mussels to attach to rocks.[2−5] This discovery has spurred numerous investigations of potential applications to the development of new adhesives and antifouling materials.[6,7] Very strong attachment of DOPA to inorganic materials such as the surface of oxidized metallic titanium has been measured using single molecule atomic force microscopy (AFM) techniques.[1] However, the extent of adsorption, the detailed mechanism of DOPA attachment, and the dependence on environmental conditions have not been established even for simple inorganic oxides.

The closest molecular analogues to DOPA that have been studied are the molecules dopamine, hydrocinnamic acid and catechol (see Supporting Information (SI)). A wide variety of studies have addressed the adsorption mechanisms and the bulk adsorption characteristics. Studies of the surface chemistry of these molecules on titanium dioxide are of interest to the development of solar cells.[8,9] UV photoemission spectroscopy, scanning tunneling microscopy, carbon K-edge NEXAFS spectroscopy, and DFT calculations of dopamine on anatase (101) and rutile (110), respectively, in the absence of water have indicated a bidentate attachment of the phenolic oxygens to one or two surface titanium atoms. In these experiments, the orientation of the molecule is approximately perpendicular to the surface. Similarly for catechol, scanning tunneling microscopy and DFT calculations have demonstrated that a bidentate attachment of the phenolic oxygens to a rutile (110) surface in vacuum enables the catechol molecules to "walk" across the surface while maintaining one inner-sphere attachment at all times and a second point of attachment involving H-bonds to surface oxygens or −OH groups.[10]

In aqueous solution, ATR-FTIR and SERS spectroscopic studies of catechol, dopamine, and hydrocinnamic acid adsorption on oxide particles have indicated inner-sphere attachment through the phenolic oxygens.[11−15] For catechol on titanium dioxide, alumina and goethite strong adsorption occurs over a wide range of pH values from 4 to about 9, and on titanium dioxide this involves the formation of a colored charge−transfer complex.[13,16−19] It has been inferred that two reactions were consistent with both adsorption and electrokinetic data[13] for

Received: December 21, 2010
Accepted: March 16, 2011
Revised: February 22, 2011
Published: April 07, 2011

catechol on titanium dioxide:

$$> TiOH^{1/3-} + H_2L^0 = > TiL^{4/3-} + H^+ + H_2O \quad (1)$$

and

$$2 > TiOH^{1/3-} + H_2L^0 = > Ti_2L^{2/3-} + 2H_2O \quad (2)$$

where H_2L^0 represents catechol and $> TiOH^{1/3-}$ represents a singly coordinated −OH group. Similar adsorption reactions are possible in principle with dopamine, hydrocinnamic acid and DOPA, but more than one surface species has not been reported, possibly because a range of pH values has not been studied.

We have studied L-DOPA adsorption on a well-characterized rutile powder over a wide range of environmental conditions. For comparison, we have also studied the adsorption of L-phenylalanine which does not contain phenolic oxygens (see SI). The data have been analyzed with the aid of a surface complexation model to establish the stoichiometry, model speciation and thermodynamic equilibrium constants for DOPA on rutile surfaces. This represents a step toward being able to predict DOPA adsorption on other solids and in compositionally more complex systems.

MATERIALS AND METHODS

Materials. All solutions and suspensions were made from Milli-Q-water (Millipore, resistance = 18.2 MΩ cm^{-1}). NaCl (Fisher BioReagents p.a., dried at 180 °C) was used to provide a constant ionic strength of 0.01 or 0.1. Stock solutions of HCl (J.T. Baker, p.a.) were standardized against tris(hydroxymethyl)-aminomethane (Trizma base, Fisher Scientific 99.9%). NaOH (J.T. Baker) solutions were standardized against these standardized HCl solutions. Stock solutions of L-phenylalanine (Sigma-Aldrich >98%) and L-DOPA (Acros Organics, 99%) were freshly prepared prior to each experiment without further purification. Ultrasonication was required to fully dissolve the amino acids. For amino acid analysis, the following chemicals were used without further purification: ninhydrin (Aldrich, 97%), 2-methoxyethanol (Sigma-Aldrich, 99.9%), acetic acid (Sigma-Aldrich, 99%), sodium acetate (Sigma-Aldrich, 99%), NaCN (Fisher), and ethanol (The Warner Graham Company, 200 proof).

The rutile sample used in the present study (obtained from Oak Ridge National Laboratory courtesy of J. Rosenqvist, D. Wesolowski, and M. Machesky) was from the same extensively cleaned and well-characterized batch previously described[20−24] with specific surface area and pH_{PPZC} of 18.1 m^2 g^{-1} and 5.4, respectively. Scanning electron microscopy (SEM) revealed needle-shaped crystals approximately 50−100 nm wide and 400−500 nm long. The most clearly visible faces are (110) parallel to the length of the crystals and (101) and (111) as terminating faces. The extent to which (101) and (111) faces may be present as steps on the (110) face is not known but is assumed in the present study to be significant because the surface functional groups for the chelating surface species hypothesized previously for glutamate based on surface complexation modeling of adsorption data and spectroscopic and quantum chemical modeling[25] do not occur on the (110) face.

EXPERIMENTAL METHODS

Quantitative adsorption of phenylalanine and DOPA on rutile was studied at 25 ± 1 °C and 1 bar using batch samples with a solid concentration of 20 g L^{-1} and a total concentration of DOPA ranging from 0.05 to 1 mM. Samples were prepared in 15 mL Falcon tubes to which precise volumes of standardized HCl or NaOH were added to each sample to achieve a range of pH values. Purified argon gas was allowed to flow through the suspensions to avoid contamination by CO_2 and O_2 from air. Preliminary experiments showed that the color of aqueous DOPA solutions changed from colorless to increasingly dark when pH was greater than 7, in agreement with previous studies.[26,27] Because of this, all our experimental DOPA adsorption data refer to pH values less than 7, whereas the adsorption of phenylalanine was studied at pH values ranging from 3 to 10. All solutions and batch samples containing DOPA were wrapped in aluminum foil in order to avoid degradation when exposed to light.

Preliminary experiments with a wide range of different amino acids indicated that the adsorption reached a steady state within the first 3 h after addition of the amino acid to a rutile suspension. The present work was based on the assumption that DOPA and phenylalanine behave in similar ways and therefore batch samples were equilibrated on a test tube rotator (Labroller II, Labnet International, Inc., H5100) for about 6 h. Longer equilibration times were avoided in order to minimize the potential oxidation of DOPA in solution. After this, the pH was measured with a combination glass electrode (Thermo-Electron, Orion 8103BNUWP) calibrated with standardized pH buffers (Fisher Scientific). Samples were centrifuged for 10 min at a relative centrifugal force of 1073*g* (Fisher Scientific accuSpin 400). The concentrations of amino acids in the supernatant were measured with UV−vis spectroscopy (Hewlett-Packard, 8452A, diode array spectrophotometer). Phenylalanine was first derivatized using the ninhydrin-labeling technique as described previously,[20] whereas DOPA was analyzed directly in the spectrophotometer without derivatization using an acetate buffer. UV-vis spectroscopy has been shown previously to be a suitable technique for quantifying aqueous concentrations of DOPA[26,27] at a wavelength of 280 nm. Hence, a calibration curve was determined for DOPA at this wavelength using an acetate buffer medium. With this method, an extinction coefficient equal to 2167 M^{-1} cm^{-1} was determined using the Beer−Lambert Law and a path length of 1 cm. A calibration curve was determined for phenylalanine at 570 nm, which yielded an extinction coefficient equal to 17,356 M^{-1} cm^{-1} using the Beer−Lambert Law and a path length of 1 cm. The difference between the initial amino acid concentration and the concentration remaining in the supernatant after equilibration was taken to correspond to the amount of amino acid adsorbed on the surface of rutile. By so doing we assumed that negligable amino acid was lost by pathways other than adsorption (e.g., through irreversible oxidation reactions).

The above assumption is supported by the following observations:

(1) All adsorption experiments referred to pH values less than 7 above which DOPA is known to oxidize.[26,27]
(2) UV−visible spectra of the supernatant aqueous solutions after adsorption showed evidence only of DOPA. The spectra contained no signs of the oxidation products of DOPA which form readily in aqueous solution at higher pH values.[27]
(3) On contacting the rutile, DOPA caused a color change for the solid from pure white to a tan color. This change is consistent with the formation of a charge transfer complex at the surface as documented in numerous studies of related molecules containing catechol entities.[15] It was reversible by addition of phosphate in equal or larger amounts than the DOPA because the phosphate adsorption almost completely prevents DOPA adsorption (SI Figure SI.2).

Table 1. Aqueous DOPA properties[a], rutile (a-TiO_2) characteristics[b] and extended triple-layer model parameters for proton, electrolyte and DOPA adsorption on rutile

reaction type	reaction	log*K*
aqueous	$DP^{3-} + H^+ = HDP^{2-}$	13.3
DOPA	$HDP^{2-} + H^+ = H_2DP^-$	9.9
equilibria	$H_2DP^- + H^+ = H_3DP^0$	8.8
	$H_3DP^0 + H^+ = H_4DP^+$	2.2
surface equilibria	hypothetical 1.0 m standard state	
$\log K_1^0$	$>TiOH + H^+ = > TiOH_2^+$	2.52
$\log K_2^0$	$>TiO^- + H^+ = > TiOH$	8.28
$\log^* K_{M^+}^0$	$>TiOH + M^+ = > TiO^-\_M^+ + H^+$	−5.6
$\log^* K_{L^-}^0$	$>TiOH + H^+ + L^- = > TiOH_2^+\_L^-$	5.0
$\log^* K^0_{(>TiOH)>Ti_3DP}$	$4 > TiOH + H_3DP = (>TiOH) > Ti_3DP + 3H_2O$	11.8(±0.2)
$\log^* K^0_{(>TiOH_2^+)>TiHDP^-}$	$2 > TiOH + H_3DP = (>TiOH_2^+) > TiHDP^- + H_2O$	6.4(±0.2)
surface equilibria	site-occupancy standard states[c]	
$\log K^\theta_{(>TiOH)>Ti_3DP}$	$>TiOH + 3 > TiOH_2^+ + H_3DP = (>TiOH) > Ti_3DP + 3H^+ + 3H_2O$	16.1 (±0.3)
$\log K^\theta_{(>TiOH_2^+)>TiHDP^-}$	$2 > TiOH_2^+ + H_3DP = (>TiOH_2^+) > TiHDP^- + 2H^+ + H_2O$	4.7(±0.3)

[a] Protonation constants from Sanaie and Haynes (2007) referring to 0.1 ionic strength. [b] Rutile properties are N_s = 3.0 sites·nm^{-2}, A_s = 18.1 m^2·g^{-1}, C_1 = 120 μF·cm^{-2}, pH_{PZC} = 5.4, ΔpK_n^θ = 6.3, $\log K_1^\theta$ = 5.25, $\log K_2^\theta$ = 8.50, $\log K_{M+}^\theta$ = 2.68, $\log K_{L-}^\theta$ = 2.48 (Jonsson et al., 2009). [c] Equilibrium constants relative to site-occupancy standard states written relative to charged surface sites calculated with

$$\log K^\theta_{(>TiOH)>Ti_3DP} = \log^* K^0_{(>TiOH)>Ti_3DP} + \log\frac{(N_s A_s)^4 C_s^3}{100} - 3pH_{PZC} + \tfrac{3}{2}\Delta pK_n^\theta$$

$$\log K^\theta_{(>TiOH_2^+)>TiHDP^-} = \log^* K^0_{(>TiOH_2^+)>TiHDP} + \log\frac{(N_s A_s)^2}{100} - 2pH_{PZC} + \Delta pK_n^\theta$$

(4) DOPA adsorbed on rutile was resuspended in phosphate solutions and UV-visible spectra showed evidence only of DOPA. A significant increase in intensity of the 280 nm band in these samples indicates that phosphate is outcompeting DOPA and causing desorption from the rutile surface without DOPA being oxidized (SI Figure SI.3).

Theoretical Surface Complexation Approach. The approach used in the present study builds on the predictive extended triple-layer model or ETLM.[20,28−33] This approach accounts for the electrical work associated with desorption of chemisorbed water molecules during inner-sphere surface complexation providing an indication of the number of inner-sphere linkages (e.g., >Ti−O−C) for the adsorbate, as well as the number of Ti surface sites involved in the reaction stoichiometry. Such information can significantly constrain the likely mode of surface attachment.

Although spectroscopic data for DOPA adsorption on oxides from aqueous solution are not available, the spectroscopic studies summarized above for the structurally related molecules catechol, dopamine, and hydrocinnamic acid provide evidence of the role of phenolic oxygens in the attachment process, although the number and type of adsorption reaction stoichiometries over wide ranges of environmental conditions remain to be established. Our approach involves iterative application of surface complexation calculations to our experimental adsorption data over a wide range of pH values, ionic strengths and ligand-to-solid ratio. This enabled testing alternative reaction stoichiometries to find the most appropriate reaction stoichiometries for DOPA on rutile in electrolyte solutions. This approach for glutamate[20] established two surface complexation reactions. The two corresponding surface species had basic features in agreement with subsequent ATR-FTIR spectroscopic and quantum chemical studies.[25] It should be emphasized that this approach requires experimental adsorption data for the surface complexation modeling over as wide a range of conditions as possible.

Our surface complexation model used the same surface protonation, electrolyte adsorption and site density parameters established in our previous studies of the adsorption of glutamate and aspartate in the rutile-NaCl system (Table 1). Aqueous p*K* values for DOPA protonation and deprotonation are also given in Table 1. Numerous studies of the aqueous p*K* values of DOPA summarized in the NIST compilation[34] refer to a range of ionic strengths without a recommended set referenced to infinite dilution. In the present study, we adopted values determined by regression of potentiometric titration data referring to an ionic strength of 0.1:[35] these p*K* values are typically within 0.1 of the values summarized by NIST and probably contribute negligible uncertainty to the modeling of our adsorption data over the pH range of 3−7.

RESULTS AND DISCUSSION

Our data for DOPA show strong adsorption, up to about 1.1 μmoles·m^{-2} (Figure 1a−d). Uncertainties in the experimental data contribute to a scatter that is typically less than about ±5%, based on the reproducibility between duplicate batch runs, as well as the stability of the readings during the UV-Vis spectroscopic measurements. Triplicate absorbance readings were performed for each sample and the small variation in concentration obtained for each sample represents the uncertainty of the instrumental analysis method itself. It can be seen in Figure 1a−d that DOPA adsorption increases with pH, particularly at low surface loadings and higher ionic strength. However, at pH values of 5−6 the adsorption tends to plateau, particularly at high surface loadings and low ionic strength (Figure 1b). This behavior is similar to published studies of catechol adsorption on TiO_2, goethite, and alumina, which also show a maximum in the adsorption above pH values of about 7 to 8 and a decrease in adsorption at higher pH values. In contrast, preliminary data for phenylalanine show consistently low adsorption on the order of about 0.03 μmoles·m^{-2} over the whole pH range from 3 to 10 (SI Table SI.2). The marked contrast between the very weak adsorption of phenylalanine and the similar adsorption patterns of DOPA and catechol strongly indicates that the adsorption of DOPA is at least in part associated

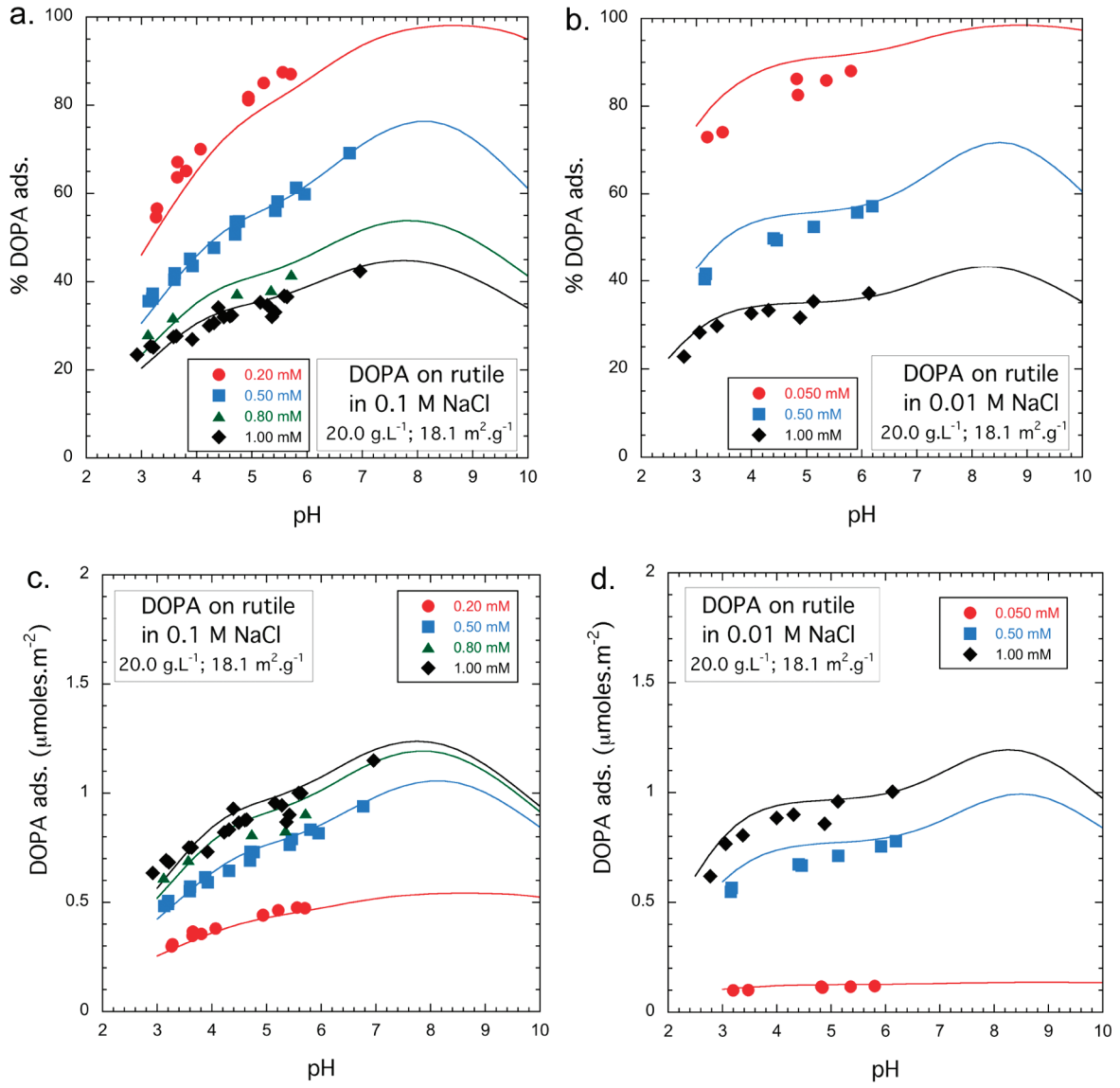

Figure 1. Adsorption of L-DOPA on rutile as a function of pH at varying ligand concentrations: in (a) and (b) % DOPA adsorbed at 0.1 and 0.01 M NaCl, respectively; in (c) and (d) DOPA adsorbed in μmol·m^{-2} at 0.1 and 0.01 M, respectively. The symbols represent experimental data. The solid curves were calculated using the surface complexation model with parameters from Table 1. Numerical values of the experimental adsorption data are given in the SI.

with attachment by the same phenolic −OH groups inferred to be responsible for the attachment of catechol.

The model curves depicted in Figure 1a−d are based on two reactions that were found to be consistent with the experimental adsorption data within the uncertainties described above:

$$4 > \mathrm{TiOH} + \mathrm{H_3DP} = (> \mathrm{TiOH}) > \mathrm{Ti_3DP} + 3\mathrm{H_2O} \quad (3)$$

and

$$2 > \mathrm{TiOH} + \mathrm{H_3DP} = (> \mathrm{TiOH_2^+}) > \mathrm{TiHDP^-} + \mathrm{H_2O} \quad (4)$$

In eqs 3 and 4 >TiOH represents a site in the 2pK model approach for titanium dioxide[36] and H_3DP represents the electrically neutral DOPA molecule which could potentially lose three protons: the two phenolic −OH protons and a proton from the amine $-NH_3^+$ group. Our conclusion that DOPA has two different ways of attaching to an oxide surface is a novel result. In addition, an important feature of eqs 3 and 4 is that four and two sites are involved, respectively. In other words, the two different surface species involve four or two points of contact of the adsorbed DOPA with the surface of rutile. This is an indication that more than just the phenolic oxygens are involved in the adsorption.

It should be emphasized that the surface complexation modeling establishes reaction stoichiometries only (eqs 3 and 4). Nevertheless, it is useful to show what the surface DOPA species might look like on a model rutile surface (Figure 2a and b). These are highly idealized representations based on fragments of the bulk structure of rutile. Both species are attached through combinations of inner-sphere and H-bonding mechanisms. It has been assumed that inner-sphere bonds between DOPA and the rutile involve terminal oxygens such as in $> \mathrm{TiOH_2^+}$. Such functional groups have been identified as the ones involved in ligand-exchange reactions for other oxyanions and mineral surfaces.[37,38]

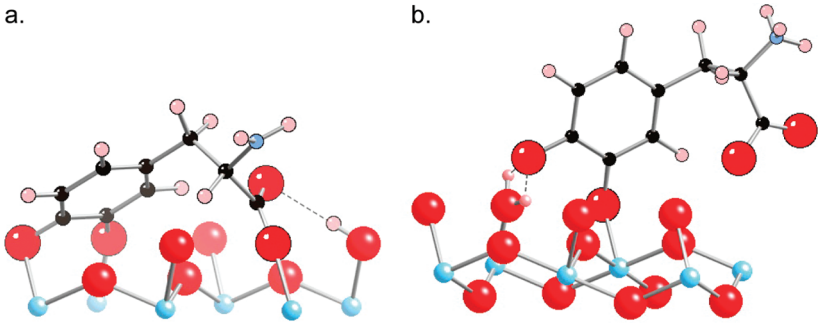

Figure 2. Surface species for DOPA on rutile consistent with surface complexation calculations (for additional species see SI). Large spheres indicate O atoms, small filled spheres C, small pale spheres H or N, and the lowermost spheres Ti at the rutile surface (to scale). Dashed lines represent H-bonds: a. "Lying down" species, (>TiOH) > Ti_3DP, four points of attachment involving three Ti−O−C bonds and one Ti−OH...O−C hydrogen bond.b. "Standing up" species, (>$TiOH_2^+$) > $TiHDP^-$, two points of attachment involving one Ti−O−C bond and one Ti−OH_2...O−C hydrogen bond.

In Figure 2a, the species (>TiOH) > Ti_3DP has three inner-sphere and one H-bond attachment. Here DOPA is "lying down" on the surface. Two of the three inner-sphere attachments involve the two phenolic oxygens the separation of which (2.78 Å) matches almost perfectly the separation of the two precursor surface > $TiOH_2^+$ groups (2.77 Å) as exposed on the ideal (101) surface. The third inner-sphere bond involves one of the carboxylate oxygens. The other carboxylate oxygen is shown as being H-bonded to a surface > TiOH group. In this example, the rutile (101) surface was used because of the very close match of the phenolic oxygen separation with the surface > $TiOH_2^+$ groups. On the ideal rutile (110) surface these groups have a greater separation (2.96 Å) which may not be as favorable for a reaction such as in eq 3.

In Figure 2b, the species (>$TiOH_2^+$) > $TiHDP^-$ has only two points of attachment to the surface. Here DOPA is "standing up" on the surface attached by an inner-sphere bond and an H-bond. Only the phenolic oxygens are involved in these bonds.

The reactions in eqs 3 and 4 correspond to the equilibrium constants

$$\log {}^{*}K^{0}_{(>TiOH)>Ti_3DP} = \frac{a_{(>\mathrm{TiOH})>\mathrm{Ti_3DP}}\, a^{3}_{\mathrm{H_2O}}}{a^{4}_{>\mathrm{TiOH}}\, a_{\mathrm{H_3DP}}} 10^{F\Delta\psi_{r,3}/2.303\mathrm{RT}} \quad (5)$$

and

$$\log {}^{*}K^{0}_{(>TiOH_2^+)>TiHDP^-} = \frac{a_{(>\mathrm{TiOH_2^+})>\mathrm{TiHDP^-}}\, a_{\mathrm{H_2O}}}{a^{2}_{>\mathrm{TiOH}}\, a_{\mathrm{H_3DP}}} 10^{F\Delta\psi_{r,4}/2.303\mathrm{RT}} \quad (6)$$

where the superscripts "*" and "0" refer to reactions written relative to >TiOH and to the hypothetical 1.0 M standard state, respectively, which applies to both aqueous and surface species.[39] The above equilibrium constants are converted to new ones referring to site occupancy standard states for the surface species as described below.

The terms involving $\Delta\psi_{r,3}$ and $\Delta\psi_{r,4}$ in eqs 5 and 6 represent the electrical work involved in the reactions given by eqs 3 and 4, respectively. In the ETLM, the electrical work includes contributions for the water dipoles coming off the surface[29] given by $\Delta\psi_r = -n_{H_2O}(\psi_0 - \psi_\beta)$, where n_{H_2O} represents the number of moles of water on the right-hand side of the reaction. In eqs 3 and 4, n_{H_2O}= 3 ($\Delta\psi_{r,3} = 0$) and n_{H_2O}= 1 ($\Delta\psi_{r,4} = \psi_0 - \psi_\beta$), respectively.

It should be emphasized that the reactions represented by eqs 3 and 4 can also be written in the following ways. Equation 3 can be written as

$$4 > \mathrm{TiOH} + \mathrm{H_3DP} = (>\mathrm{TiOH})_2 > \mathrm{Ti_2HDP} + 2\mathrm{H_2O} \quad (7)$$

$$4 > \mathrm{TiOH} + \mathrm{H_3DP} = (>\mathrm{TiOH})_3 > \mathrm{TiH_2DP} + \mathrm{H_2O} \quad (8)$$

or

$$4 > \mathrm{TiOH} + \mathrm{H_3DP} = (>\mathrm{TiOH})_4\_\mathrm{H_3DP} \quad (9)$$

and eq 4 can be written as

$$>\mathrm{Ti(OH)_2} + >\mathrm{TiOH} + \mathrm{H_3DP} = >\mathrm{Ti} > \mathrm{Ti(OH_2^+)DP^-} + 2\mathrm{H_2O} \quad (10)$$

or

$$2 > \mathrm{TiOH} + \mathrm{H_3DP} = (>\mathrm{TiOH}) > \mathrm{TiOH_2^+}\_\mathrm{H_2DP^-} \quad (11)$$

Diagrams of the surface species are given in the SI. Equations 7−9 are of the same form as eq 3 and have the same values of log$K$ and $\Delta\psi_r$. However, instead of three inner-sphere bonds there are either two, one or zero, respectively, in eqs 7−9. Equations 10 and 11 have the same form as eq 4 and the same values of log$K$ and $\Delta\psi_r$. However, the surface species in eq 10 involves two inner-sphere and one H-bond, whereas in eq 11 only H-bonding is involved. These alternatives to eqs 3 and 4 cannot be distinguished by surface complexation modeling alone.

Published AFM and spectroscopic studies permit distinguishing between some of the above surface species. A role for an inner-sphere bonding mechanism for DOPA and related molecules on rutile is suggested by the strong attachment of DOPA to titanium dioxide measured using single molecule AFM.[1] This is supported by results for catechol, dopamine and hydrocinnamic acid (SI Figure SI.1a−e) attachment to titanium dioxide based on adsorption, electrokinetic, ATR-FTIR, SERS and UV−vis spectroscopic studies.[11−13,15,40,41] Consequently, at least some of the attachment points of DOPA to rutile must be inner-sphere. This eliminates eqs 9 and 11 as they only involve H-bonds. The most relevant adsorption reactions are likely eqs 3 and either eqs 4 or 10 because they have the fewest H-bonds.

The solid curves in Figure 1 represent regression calculations using the reactions in eqs 3 and 4. In these calculations, a site density of 3.0 (±0.5) sites nm^{-2} was found to be the most appropriate site density, as in the case of glutamate and aspartate on the same rutile sample.[20,32] This site density is consistent with the idea that adsorption takes place on (101) or (111) steps on the (110) surface of rutile.

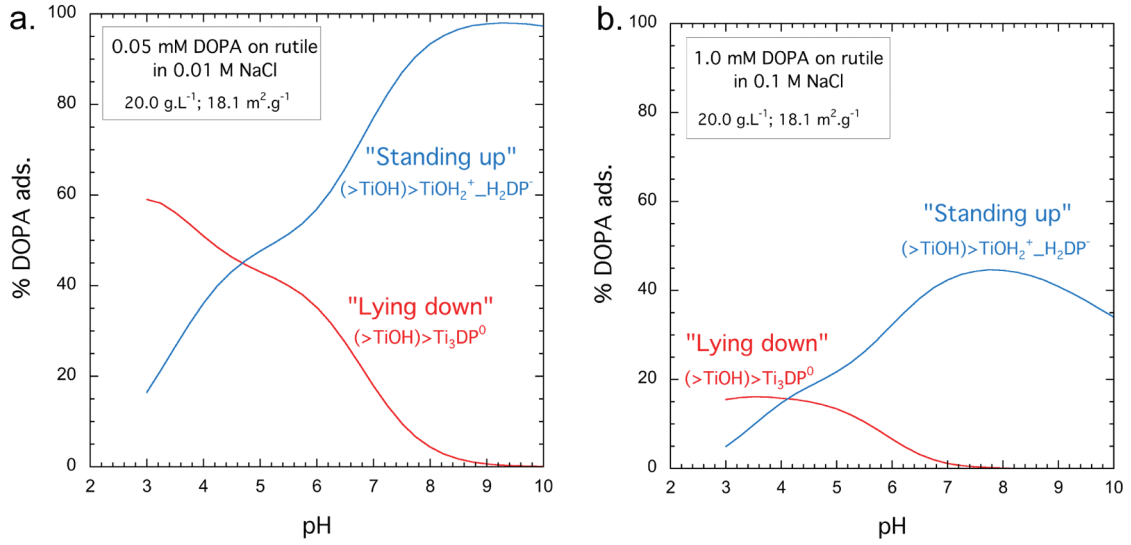

Figure 3. Predicted surface speciation of DOPA on rutile as a function of environmental conditions. Names refer to Figure 2 and eqs 3 and 4.

Equilibrium constants for DOPA adsorption ($\log{}^{*}K^{0}_{(>TiOH)>Ti_3DP}$ and $\log{}^{*}K^{0}_{(>TiOH_2^{+})>TiHDP^{-}}$, Table 1) have estimated uncertainties of ±0.2 in the log values. Based on the estimated experimental uncertainties and the uncertainties in the regression parameters, the calculated curves in the figures show relatively small discrepancies with the experimental data. Clearly, the two reactions are sufficient to describe DOPA adsorption on rutile as a function of pH, ligand-to-solid ratio and ionic strength. The regression equilibrium constants were converted to values of $\log K^{\theta}_{(>TiOH)>Ti3DP}$ and $\log K^{\theta}_{(>TiOH_2^{+})>TiHDP^{-}}$ referring to site-occupancy standard states and referenced to $>TiO^{-}$ using the equations and values of N_s (site density), A_s (BET surface area), C_s (solid concentration), pH_{PPZC}, and ΔpK_n^{θ} given in Table 1. These equilibrium constants are useful for predicting the binding of DOPA on different oxides.

A qualitative test of the reaction stoichiometries proposed in eqs 3 and 4 involves prediction of the migration of the isoelectric point (IEP) of rutile with increasing DOPA concentrations. Although this behavior has not been measured for DOPA, it has been measured for catechol on titanium dioxide and alumina.[13,16,18] On both solids a substantial migration to lower IEP values takes place with increasing catechol adsorption. For example, on titanium dioxide the IEP migrates from 6.5 to about 5.5 for a 5.0 mM solution of catechol (solid concentration unspecified). Strong changes such as this are often inferred to correspond to inner-sphere surface complexation. Using our surface complexation model for DOPA, and assuming that the model value of $\psi_d = 0$ represents the IEP of rutile,[42] results in a prediction that the IEP decreases from 5.4 to 4.4 for a 5.0 mM DOPA solution (20 $g \cdot L^{-1}$). In our model, this decrease in the isoelectric point arises entirely from the reaction in eq 4. The agreement of this result with the catechol data supports the importance of the reaction in eq 4 for DOPA adsorption.

The predicted surface speciation of DOPA on rutile is shown in Figure 3a and b as functions of pH over a range of surface coverages and ionic strengths. The surface species "lying down", (>TiOH) > Ti_3DP, is predicted to be the predominant one at pH values less than about 4.5, depending on the amount of DOPA in the system. The surface species "standing up", ($>TiOH_2^{+}$) > $TiHDP^{-}$, is predominant at higher pH values. The proportion of the two is only weakly affected by ionic strength and the amount of DOPA in the system. The weak ionic strength dependence of the adsorption is also a possible indication of inner-sphere surface complexation. Comparing the "standing up" species ($>TiOH_2^{+}$) > $TiHDP^{-}$ in eq 4 with the adsorption mechanisms proposed for catechol on titanium dioxide suggests similarities with eq 2.

Overall the experimental measurements and theoretical calculations described above for DOPA provide a novel picture of the adsorption behavior of DOPA on the rutile surface in electrolyte solutions over a range of pH, ionic strength and surface loading. Previous studies of DOPA and dopamine molecules have focused on only one mode of attachment to surfaces without information on how the attachment might change with environmental conditions. Our results show that DOPA forms two surface species, the proportions of which vary strongly as a function of pH and are weak functions of ionic strength and surface loading. One species involving four attachment points, "lying down" on the surface, is important only at pH less than about 4.5, the other species can be thought of as "standing up" on the surface and is predicted to adsorb strongly up to pH values of 9−10. It has only two attachment points via the phenolic oxygens. At least one of the DOPA attachment points for each species are inner-sphere. The others are likely H-bonded.

It is interesting to speculate on the relevance of the present study to understanding the role of DOPA molecules in bioadhesion proteins. Because the DOPA in these proteins is linked by peptide bonds to other amino acids, the DOPA side chain is the relevant part of the molecule. Some of these have been suggested to be cross-linked to neighboring adsorbed proteins by cations such as Fe^{3+} and Ca^{2+}.[5] However, if other DOPA side chains are free to attach to mineral surfaces, the "standing up" species (eq 4 and Figure 2b) may be the most relevant for the DOPA attachment mechanism. The fact that similar attachments in the case of catechol on the rutile (110) surface enable the catechol to "walk" across the surface[10] may possibly be useful in developing reversible adhesives in water under the appropriate pH conditions.

■ ASSOCIATED CONTENT

Supporting Information. Diagrams of the structures of organic molecules referred to in the present paper are given. UV-visible spectra of aqueous solutions of DOPA and phosphate desorption experiments are discussed. Pictures of additional surface DOPA complexes are provided. Adsorption data for DOPA and phenylalanine are tabulated. This material is available free of charge via the Internet at http://pubs.acs.org.

■ AUTHOR INFORMATION

Corresponding Author
*Phone: 410-516-8568; fax: 410-516-7933; e-mail: sver@jhu.edu.

■ ACKNOWLEDGMENT

We greatly appreciate discussions with and assistance in the laboratory from G. D. Cody, H. J. Cleaves, N. Lee and K. Klochko. We also thank the four reviewers for their comments. Financial support was provided by a NSF-NASA Collaborative Research Grant to Johns Hopkins University and the Carnegie Institution for Science. D. A. Sverjensky acknowledges DOE Grant DE-FG02-96ER-14616. S. Bahri acknowledges support from the National Science Foundation-Research Experience for Undergraduates Program at the Geophysical Laboratory (S. Gramsch).

■ REFERENCES

(1) Lee, H.; Scherer, N. F.; Messersmith, P. B. Single-molecule mechanics of mussel adhesion. *Proc. Natl. Acad. Sci.* **2006**, *103*, 12999–13003.

(2) Guvendiren, M.; Brass, D. A.; Messersmith, P. B.; Shull, K. R. Adhesion of DOPA-functionalized model membranes to hard and soft surfaces. *J. Adhes.* **2009**, *85* (9), 631–645.

(3) Waite, J. H., Reverse engineering of bioadhesion in marine mussels. In *Bioartificial Organs Ii: Technology, Medicine, and Materials*; Hunkeler, D., Prokop, A., Cherrington, A. D., Rajotte, R. V., Sefton, M., Eds.; New York Acad Sciences: New York, 1999; Vol. 875, pp 301−309.

(4) Lin, Q.; Gourdon, D.; Sun, C. J.; Holten-Andersen, N.; Anderson, T. H.; Waite, J. H.; Israelachvili, J. N. Adhesion mechanisms of the mussel foot proteins mfp-1 and mfp-3. *Proc. Natl. Acad. Sci. U. S. A.* **2007**, *104*, (10), 3782-3786.

(5) Hwang, D. S.; Zeng, H. B.; Masic, A.; Harrington, M. J.; Israelachvili, J. N.; Waite, J. H. Protein- and metal-dependent interactions of a prominent protein in mussel adhesive plaques. *J. Biol. Chem.* **2010**, *285* (33), 25850–25858.

(6) Statz, A. R.; Meagher, R. J.; Barron, A. E.; Messersmith, P. B. New peptidomimetic polymers for antifouling surfaces. *J. Am. Chem. Soc.* **2005**, *127*, 7972–7973.

(7) Lee, H.; Lee, B. P.; Messersmith, P. B. A reversible wet/dry adhesive inspired by mussels and geckos. *Nature* **2007**, *448* (7151), 338–U4.

(8) Li, S.-C.; Wang, J.-g.; Jacobson, P.; Gong, X. Q.; Selloni, A.; Diebold, U. Correlation between bonding geometry and band gap states at organic and inorganic interfaces: Catechol on rutile TiO2(110). *J. Am. Chem. Soc.* **2009**, *131* (3), 980–984.

(9) Syres, K.; Thomas, A.; Bondino, F.; Malvestuto, M.; Gratzel, M. Dopamine adsorption on anatase TiO_2 (101): A photoemission and NEXAFS spectroscopy study. *Langmuir* **2010**, *26* (18), 14548–14555.

(10) Li, S. C.; Chu, L. N.; Gong, X. Q.; Diebold, U. Hydrogen bonding controls the dynamics of catechol adsorbed on a TiO_2 (110) surface. *Science* **2010**, *328* (5980), 882–884.

(11) Araujo, P. Z.; Morando, P. J.; Blesa, M. A. Interaction of catechol and gallic acid with titanium dioxide in aqueous suspensions. 1. Equilibrium studies. *Langmuir* **2005**, *21*, 3470–3474.

(12) Gulley-Stahl, H.; Hogan, I., P. A.; Schmidt, W. L.; Wall, S. J.; Buhrlage, A.; Bullen, H. A. Surface complexation of catechol to metal oxides: An ATR-FTIR, adsorption, and dissolution study. *Environ. Sci. Technol.* **2010**, *44*, 4116–4121.

(13) Rodriguez, R.; Blesa, M. A.; Regazzoni, A. E. Surface complexation at the TiO2 (anatase)/aqueous solution interface: Chemisorption of catechol. *J. Colloid Interface Sci.* **1996**, *177*, 122–131.

(14) Lana-Villarreal, T.; Rodes, A.; Perez, J. M.; Gomez, R. A spectroscopic and electrochemical approach to the study of the interactions and photoinduced electron transfer between catechol and anatase nanoparticles in aqueous solution. *J. Am. Chem. Soc.* **2005**, *127* (36), 12601–12611.

(15) Hurst, S. J.; Fry, H. C.; Goztola, D. J.; Rajh, T. Utilizing chemical Raman enhancement: A route for metal oxide support-based biodetection. *J. Phys. Chem.* **2011**, *115*, 620–630.

(16) Laucournet, R.; Pagnoux, C.; Chartier, T.; Baumard, J. F. Catechol derivatives and anion adsorption onto alumina surfaces in aqueous media: influence on the electrokinetic properties. *J. Eur. Ceram. Soc.* **2001**, *21*, 869–878.

(17) Evanko, C. R.; Dzombak, D. A. Surface complexation modeling of organic acid sorption to goethite. *J. Colloid Interface Sci.* **1999**, *214*, 189–206.

(18) Hidber, P. C.; Graule, T. J.; Gauckler, L. J. Influence of the dispersant structure on properties of electrostatically stabilized aqueous alumina suspensions. *J. Eur. Ceram. Soc.* **1997**, *17*, 239–249.

(19) Eisenthal, K. B. Second harmonic spectroscopy of aqueous nano- and microparticle interfaces. *Chem. Rev.* **2006**, *106* (4), 1462–1477.

(20) Jonsson, C. M.; Jonsson, C. L.; Sverjensky, D. A.; Cleaves, H. J., II; Hazen, R. M. Attachment of l-Glutamate to rutile (α-TiO_2): A potentiometric, adsorption, and surface complexation study. *Langmuir* **2009**, *25*, 12127–12135.

(21) Machesky, M.; Wesolowski, D. J.; Palmer, D. A.; Ichiro-Hayashi, K. Potentiometric titrations of rutile suspensions to 250°C. *J. Colloid Interface Sci.* **1998**, *200*, 298–309.

(22) Ridley, M. K.; Machesky, M. L.; Palmer, D. A.; Wesolowski, D. J. Potentiometric studies of the rutile-water interface: hydrogen-electrode concentration-cell versus glass-electrode titrations. *Colloids Surf.* **2002**, *204*, 295–308.

(23) Ridley, M. K.; Machesky, M. L.; Wesolowski, D. J.; Palmer, D. A. Calcium adsorption at the rutile-water interface: A potentiometric study in NaCl media to 250 degrees C. *Geochim. Cosmochim. Acta* **1999**, *63*, 3087–3096.

(24) Ridley, M. K.; Machesky, M. L.; Wesolowski, D. J.; Palmer, D. A. Surface complexation of neodymium at the rutile-water interface: A potentiometric and modeling study in NaCl media to 250°C. *Geochim. Cosmochim. Acta* **2005**, *69*, 63–81.

(25) Parikh, S. J.; Kubicki, J. D.; Jonsson, C. M.; Jonsson, C. L.; Hazen, R. M.; Sverjensky, D. A.; Sparks, D. L. Evaluating glutamate and aspartate binding mechanisms to rutile (⟨-TiO_2) via ATR-FTIR spectroscopy and quantum chemical calculations. *Langmuir* **2010**, (in review).

(26) Hamada, Y.; Rogers, C. Interaction of L-3,4-dihydroxyphenylalanine (L-DOPA) as a coordinating ligand with a series of metal ions; reaction of L-DOPA. *J. Coord. Chem.* **2007**, *20*, 2149–2163.

(27) Barreto, W. J.; Ponzoni, S.; Sassi, P. A Raman and UV-Vis study of catecholamines oxidized with Mn(III). *Spectrochim. Acta* **1999**, *55*, 65–72.

(28) Fukushi, K.; Sverjensky, D. A. A surface complexation model for sulfate and selenate on iron oxides consistent with spectroscopic and theoretical molecular evidence. *Geochim. Cosmochim. Acta* **2007**, *71*, 1–24.

(29) Sverjensky, D. A.; Fukushi, K. Anion adsorption on oxide surfaces: Inclusion of the water dipole in modeling the electrostatics of ligand exchange. *Environ. Sci. Technol.* **2006**, *40*, 263–271.

(30) Sverjensky, D. A.; Fukushi, K. A predictive model (ETLM) for As(III) adsorption and surface speciation on oxides consistent with spectroscopic data. *Geochim. Cosmochim. Acta* **2006**, *70*, 3778–3802.

(31) Sverjensky, D. A.; Jonsson, C. M.; Jonsson, C. L.; Cleaves, H. J.; Hazen, R. M. Glutamate surface speciation on amorphous titanium dioxide and hydrous ferric oxide. *Environ. Sci. Technol.* **2008**, *42*, 6034–6039.

(32) Jonsson, C. M.; Jonsson, C. L.; Estrada, C.; Sverjensky, D. A.; Cleaves, H. J.; Hazen, R. M. Adsorption of L-aspartate to rutile (alpha-TiO_2): Experimental and theoretical surface complexation studies. *Geochim. Cosmochim. Acta* **2010**, *74* (8), 2356–2367.

(33) Sahai, N.; Sverjensky, D. A. GEOSURF: A computer program for forward modeling of adsorption on mineral surfaces in aqueous solution. *Comp. Geosci.* **1998**, *24*, 853–873.

(34) Smith, R. M.; Martell, A. E. *NIST Critically Selected Stability Constants of Metal Complexes Database*; 46; U. S. Department of Commerce, Technology Administration, May, 2004, 2004.

(35) Sanaie, N.; Haynes, C. A. Modeling I-dopa purification by chiral ligand-exchange chromatography. *Aiche Journal* **2007**, *53* (3), 617–626.

(36) Connor, P. A.; Dobson, K. D.; McQuillan, A. J. Infrared spectroscopy of the TiO2/aqueous solution interface. *Langmuir* **1999**, *15* (7), 2402–2408.

(37) Catalano, J. G.; Zhang, Z.; Fenter, P.; Bedzyk, M. J. Inner-sphere adsorption geometry of Se(IV) at the hematite (100)-water interface. *J. Colloid Interface Sci.* **2006**, *297*, 665–671.

(38) Catalano, J. G.; Zhang, Z.; Park, C.; Fenter, P.; Bedzyk, M. J. Bridging arsenate surface complexes on the hematite (012) surface. *Geochim. Cosmochim. Acta* **2007**, *71*, 1883–1897.

(39) Sverjensky, D. A. Standard states for the activities of mineral surface-sites and species. *Geochim. Cosmochim. Acta* **2003**, *67*, 17–28.

(40) Connor, P. A.; Dobson, K. D.; McQuillan, A. J. New sol-gel attenuated total-reflection infrared spectroscopic method for analysis of adsorption at metal-oxide surfaces in aqueous-solutions - Chelation of TiO_2, ZrO_2, and Al_2O_3 Surfaces by catechol, 8-quinolinol, and acetylacetone. *Langmuir* **1995**, *11* (11), 4193–4195.

(41) Ashurst, K. G.; Hancock, R. D. Characterization of inner- and outer-sphere complexes by thermodynamics and absorption spectra. Part 2. Chloro-complexes of Copper(II). *J. Chem. Soc. Dalton* **1981**, 245–250.

(42) Sverjensky, D. A. Prediction of surface charge on oxides in salt solutions: revisions for 1:1 (M^+L^-) electrolytes. *Geochim. Cosmochim. Acta* **2005**, *69*, 225–257.